NASA CR-54702
Cosmic, Inc. Report No. 169

INVESTIGATION OF CHARGED COLLOID BEAMS FOR ELECTROSTATIC PROPULSION

GPO PRICE $ _____
CFSTI PRICE(S) $ 3.00
Hard copy (HC) 3.00
Microfiche (MF) .65
ff 653 July 65

by

D. Gignoux and H. Anton

prepared for

NATIONAL AERONAUTICS AND SPACE ADMINISTRATION

CONTRACT NAS 3-7924

FACILITY FORM 602
N67-26640 (ACCESSION NUMBER)
54 (PAGES)
CR-54702 (NASA CR OR TMX OR AD NUMBER)
(THRU) 1
(CODE)
(CATEGORY) 11

COSMIC, INC
4847 Cordell Avenue
Bethesda, Maryland 20014

NOTICE

This report was prepared as an account of Government sponsored work. Neither the United States, nor the National Aeronautics and Space Administration (NASA), nor any person acting on behalf of NASA:

A.) Makes any warranty or representation, expressed or implied, with respect to the accuracy, completeness, or usefulness of the information contained in this report, or that the use of any information, apparatus, method, or process disclosed in this report may not infringe privately owned rights; or

B.) Assumes any liabilities with respect to the use of, or for damages resulting from the use of any information, apparatus, method or process disclosed in this report.

As used above, "person acting on behalf of NASA" includes any employee or contractor of NASA, or employee of such contractor, to the extent that such employee or contractor of NASA, or employee of such contractor prepares, disseminates, or provides access to, any information pursuant to his employment or contract with NASA, or his employment with such contractor.

Requests for copies of this report should be referred to:

National Aeronautics and Space Administration
Office of Scientific and Technical Information
Attention: AFSS-A
Washington, D. C. 20546

NASA CR-54702
Cosmic, Inc. Report No. 165

F I N A L R E P O R T

INVESTIGATION OF CHARGED COLLOID BEAMS FOR ELECTROSTATIC PROPULSION

by

D. Gignoux and H. Anton

prepared for

NATIONAL AERONAUTICS AND SPACE ADMINISTRATION

May 1967

CONTRACT NAS 3-7924

Technical Management
NASA Lewis Research Center
Cleveland, Ohio
Electric Propulsion Office
Peter Ramins

COSMIC, INC.
4847 Cordell Avenue
Bethesda, Maryland 20014

ACKNOWLEDGMENTS

This investigation was made possible through the sponsorship of the National Aeronautics and Space Administration, Lewis Research Center. Researchers of this company who participated in the program wish to express their appreciation to the personnel of the Spacecraft Technology Division, in particular, Mssrs. David Lockwood, John Ferrante and Peter Ramins. The valuable guidance and many helpful suggestions of Mr. John Ferrante on this and antecedent programs is gratefully acknowledged.

TABLE OF CONTENTS

SUMMARY

A facility for testing charge colloid sources has been built. The pumping speed in the vacuum chamber is sufficient to make possible operation with beams of glycerol up to several milligrams/second. Propellants consisting of mixtures of glycerol or Octoil with agents intended to increase the conductivity of the liquid have been tried in the system. Instrumentation adequate to measure beam currents, mass flow and thrust has been developed and built, and is working satisfactorily. A spinning nozzle was used for most tests with the propellant atomized at its edge. The maximum values obtained with glycerol were: Charge-to-mass ratio, 2,000 coulomb/kilogram; current, 2 milliamperes; thrust, 125 milligrams. On most tests, the efficiency was 25 percent. It has been determined that colloids of this type are charged by a corona-like mechanism. Some tests with the liquid coming through a hollow needle instead of a nozzle led to the same conclusion.

LIST OF FIGURES

1. INTRODUCTION

Throughout history, most means of locomotion have been developed and refined while actually in use. Electric thrustors, on the other hand, have not yet been submitted to the test of actual usage. For this reason, there exists at the present time a proliferation of proposed thrustors, and the merits of one versus the other are often the subject of conjectural debate. The first realization of a working electrostatic thrustor in the U. S. A. is the result of work on ion sources which reaches back to the 1920's. Thanks to this long history, the operation of ion sources is fairly well understood and the technological problems presented by ion thrustors are, if not all resolved, at least isolated and known. With this background in mind, it appears that one can extrapolate or predict the performance and the problems of future ion thrustors.

We shall not attempt in this brief introduction to analyze the problems presented by ion thrustors. Instead, we shall review them qualitatively in the light of the advantages which the colloidal thrustors may present over ion thrustors. We shall, in this introduction, limit ourselves to qualitative arguments. The first comparison can be made in terms of efficiency defined as the ratio of the power of an ideal engine of the same thrust and mass flow to the power of the actual engine. This is not the case with colloid sources which are, at present, still not completely understood.

The motivation for undertaking development of a colloid thrustor is that it presents potential advantages over ion engines, in particular, regarding efficiency. All ion engines exhibit the same trend: a decrease in efficiency for a decrease in specific impulse (Reference 1). On the other hand, colloid sources of the type proposed here may have an efficiency that is independent of the specific impulse. It was, therefore, the goal of the work reported herein to measure this efficiency.

The colloid engine may be considered as an electrostatic engine in which a difference of potential is utilized to accelerate, not ions, but multimolecular charged particles to a high velocity. The charging of small solid and liquid particles has been attempted by bombardment, charge attachment, corona charging during condensation, and by induction. The type of charging with which we will be concerned here is due to a mechanism which will be described later in this report and for which no satisfactory theoretical explanation as yet exists.

In this method of charging, a liquid is introduced at a point in which there is an intense electric field. Charging then occurs simultaneously with the decomposition of the liquid into small droplets. In the system discussed in this report, the liquid is presented in the form of a thin film to an edge submitted to an intense electric field. On a microscopic scale, this system is analogous to that of other experimenters who have utilized a porous wedge, or capillary tubes. Obtaining the flow of the liquid towards the edge by utilizing a spinning nozzle as shown in Figure 1 presents the advantage that the mass flow of liquid can be controlled throughout a wide range, and furthermore, the long circumference of the nozzle permits operation with a much higher mass flow than is possible with other methods such as, say an array of needles. This results in higher measurable quantities.

Previous work with this type of nozzle (Reference 2) has been possible only with liquids which produce a very small quantity of a vapor in the chamber.

In this report, the construction of a large chamber with a relatively high pumping capability is described. Measurements of colloid beams, including total thrust, are then reported.

2. THE EXPERIMENTAL EQUIPMENT

The facility required to test a small colloid beam is essentially a vacuum chamber with adequate instrumentation. Requirements are somewhat more stringent than ion engine testing facilities because the voltages used are higher (up to 100,000 volts), and the pumping speed must be very high to overcome the effects of propellant evaporation. The propellants suitable for the production of colloids by this method are obviously chosen for their low vapor pressure. They all, however, evaporate to some extent in the vacuum chamber before or during spraying. They also vaporize when they impact at high velocity on the target.

2.1 General Configuration

As can be seen in Figure 1, an intense electric field is maintained at the edge of the nozzle by means of a ring-like electrode called the extractor. The edge of the nozzle is very sharp, so that compared to the radius of curvature of the edge of the nozzle, the extractor is at a great distance. The result of this geometry is that the position of the extractor does not influence to a significant degree the field configuration in the immediate vicinity of the nozzle. This configuration is, in fact, primarily determined by the shape of the nozzle itself. As the liquid droplets acquire most of their ultimate velocity within a short distance from the nozzle, their trajectories will be little influenced by the extractor and will tend to be concentrated in a cone extending from the nozzle toward the collector (Figure 1). As will be described in Section 2.4, several types of collectors have been used during the program. The one shown in Figure 1 consists of a screen and a metal target which act as a thrust measuring plate. We shall now describe, in turn, all the components of the system.

2.2 Nozzle

The nozzles that have been used (Figures 2 and 3) all have internal conical shapes. As shown in Figure 3, the recessed areas in the front and back of the nozzle are connected by a number of holes. In this manner, the liquid may be fed to the back of the nozzle, equalized circumferentially by the rotating motion of the nozzle, and then transferred to the forward section through the holes.

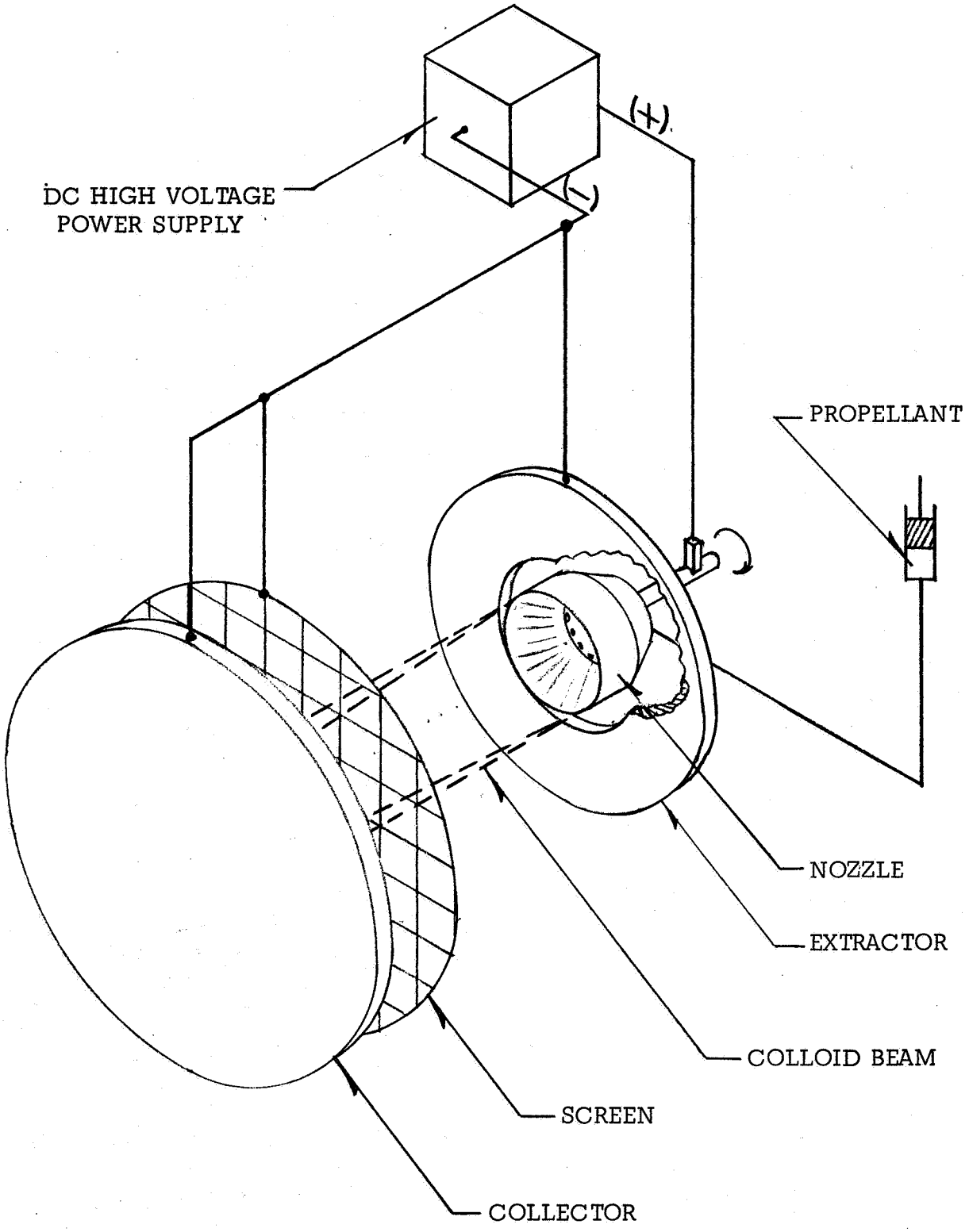

Figure 1. Principle of Operation of Spinning Nozzle Source of Charged Colloid Beam

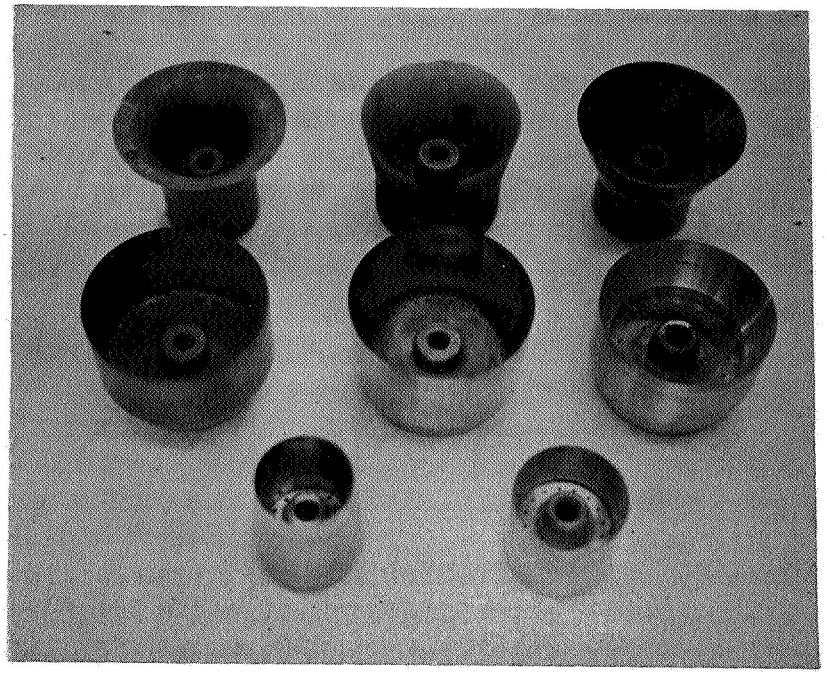

Figure 2. View of Several Nozzles

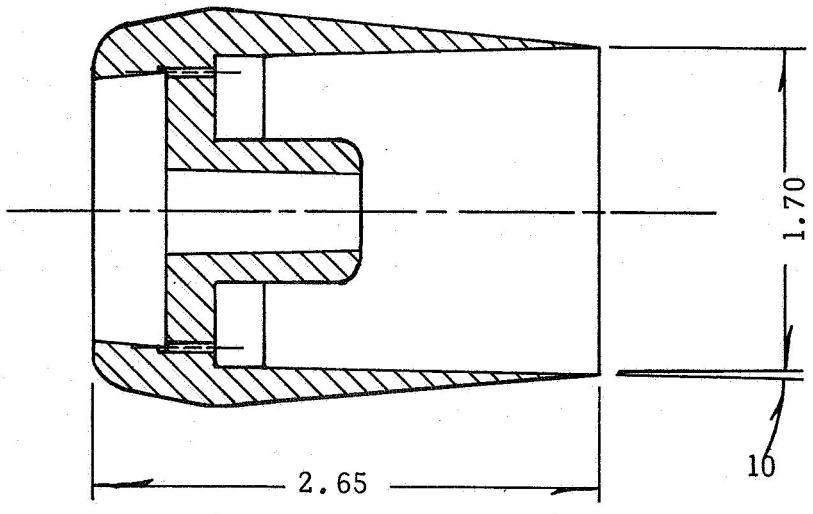

Figure 3. View of the 1.7-Inch Nozzle

Nozzles of aluminum, copper and stainless steel have been used with success. Nozzles made of insulating material have been tried in previous programs and have been found unsatisfactory. The model that has given the best results is shown in Figure 3. It has very little flare (being almost cylindrical in shape). Before tests, the edge of the nozzle is honed to a very fine edge.

2.3 Nozzle Mounting and Extractor

One of the features of the system which complicated the design of the nozzle support assembly is that the nozzle, in addition to being rotated, must be maintained at a high potential with respect to ground. The insulating mounting of the nozzle is shown in Figures 4, 5, and 6. The nozzle shaft rotates in bearings which are mounted on a platform supported by insulating teflon spacers. It is connected to the drive system by means of an insulating coupling. The magnetic drive system is a modification of that used in a previous work and is adequately described in Reference 3. The extractor is a ring with a carefully polished inside diameter and is attached to the nozzle supporting plate by means of three insulating spacers. It is connected to ground through an ammeter. Nozzle-extractor spacings have varied between $\frac{1}{8}$ and $\frac{1}{2}$ inch.

2.4 Collector

In the initial phases of the program, the beam was made to strike a solid collector as shown in Figure 7. The beam hits the collector in a ring pattern concentric with the collector so that a number of windows could be cut to obtain unbiased samples of the droplet population of the beam. In Figure 7, two such windows are shown. One window was utilized for thrust measurements (Figure 8). Another window was provided to be used for other beam sampling requirements such as the determination of the charge-to-mass ratio distribution of the droplets by menas of a quadrupole mass spectrometer.

Ideally, with perfect beam symmetry, it would be possible to obtain beam mass flow by multiplying the total mass flow by the ratio of the cross-section of the target to the cross-section of the beam. However, comparison of such calculated mass flow with the measured mass flow collected on the target using a liquid that evaporates only slightly in vacuum did show discrepancy between the "measured" and "calculated" values. To resolve this problem, it was decided to build a target large enough to intercept the entire beam.

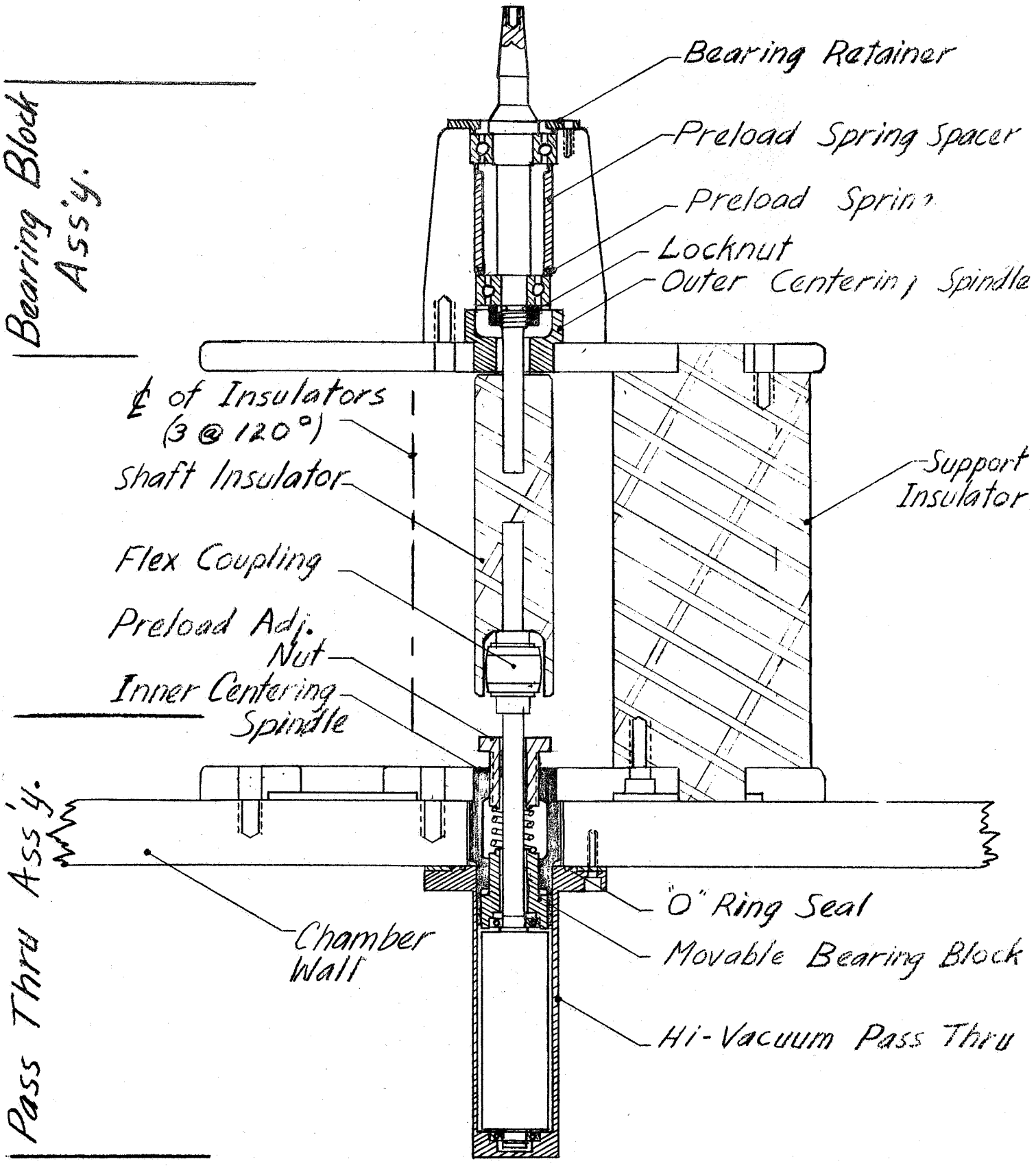

Figure 4. Assembly Drawing of Nozzle Mounting System

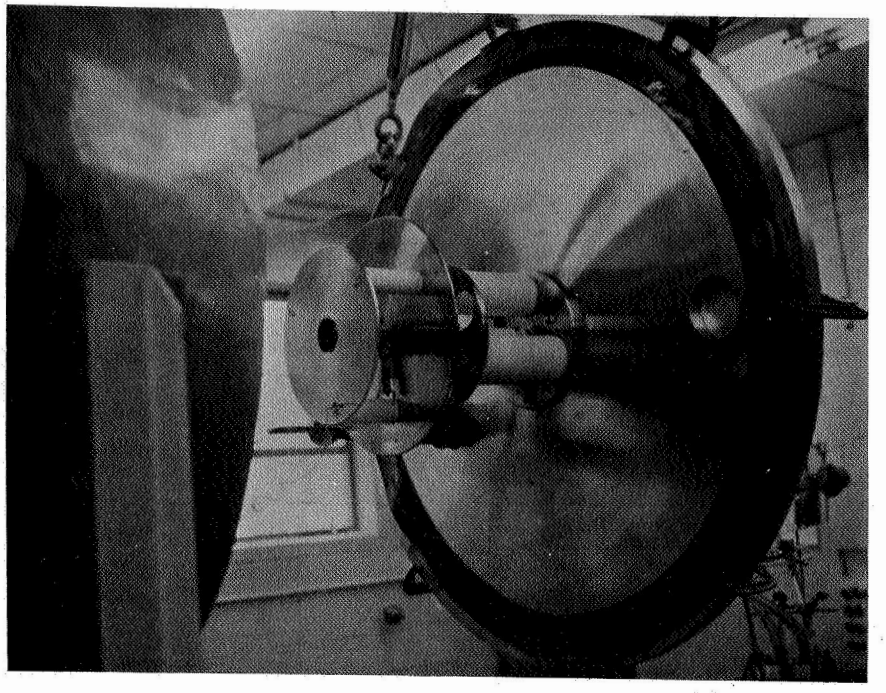

Figure 5. 1.7-inch Nozzle and Nozzle Mounting

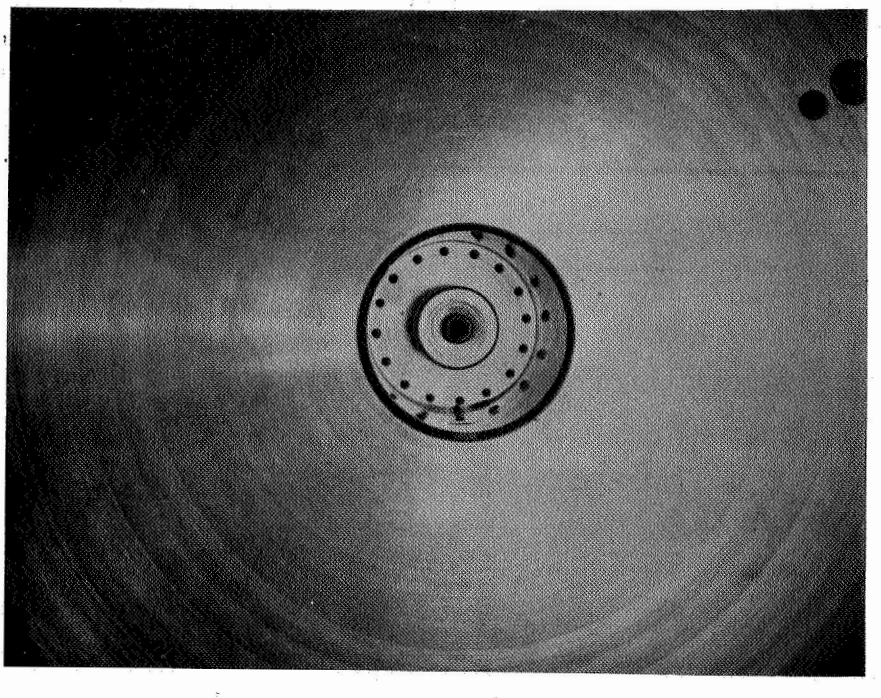

Figure 6. Closeup View of 1.7-inch Nozzle and Extractor

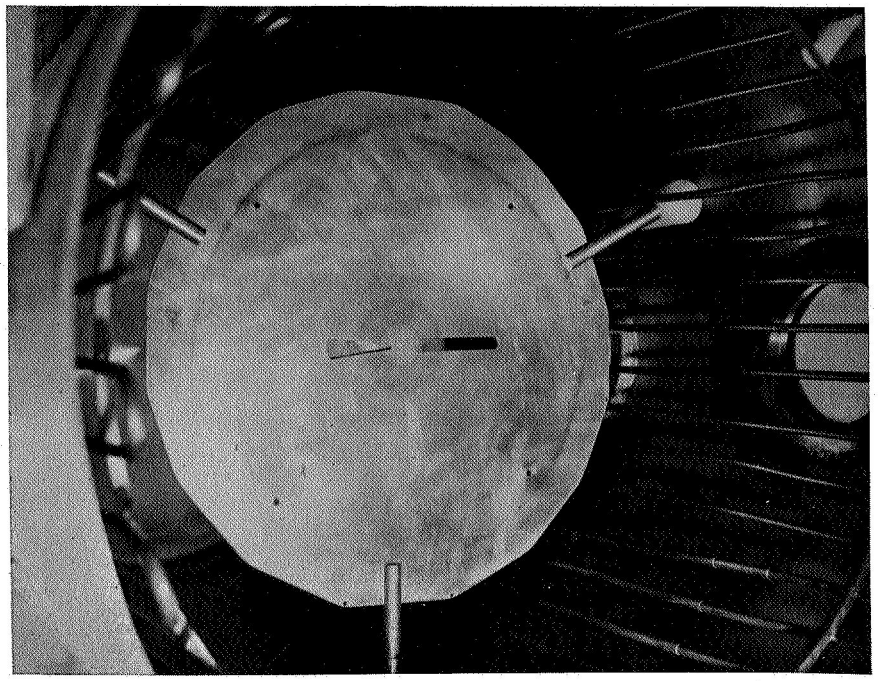

Figure 7. Chamber with Collector and Windows Showing Beam Impact.

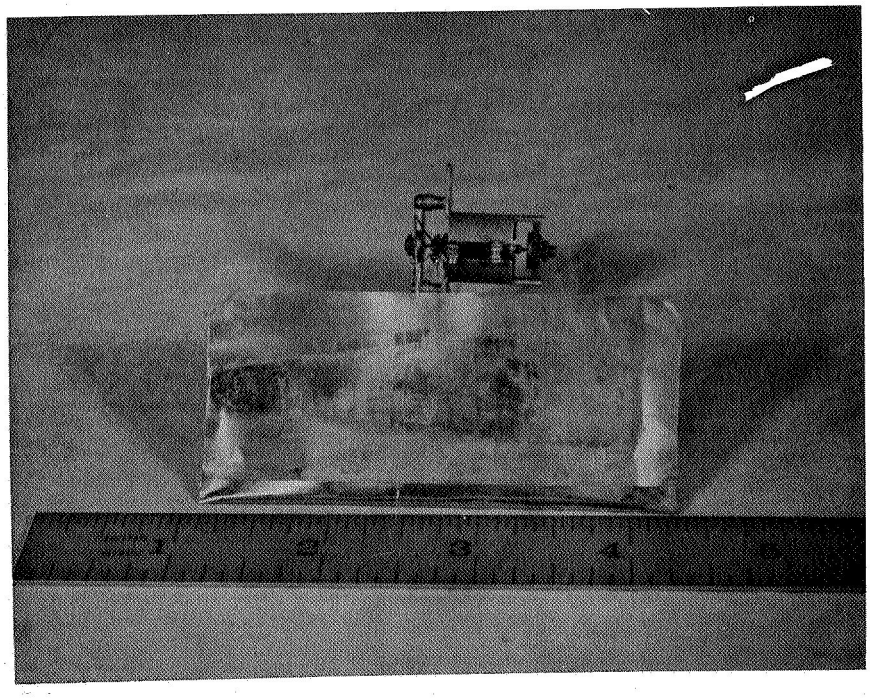

Figure 8. Thrust Measuring Plate Placed Behind Window of Figure 7 after 2 one-hour tests with a 300 to 600 coulomb/kilogram beam. During one test, the beam interception was limited to the left side of the plate which shows the most erosion.

2.5 Full-Beam Target

A full-beam target was built as shown in Figures 9 and 10. In front of the target is placed a screen which can be biased with respect to the target to prevent, if necessary, the emission of secondary electrons from the target and, more importantly, to prevent the electric field from affecting the target and therefore rendering inaccurate the thrust measurements.

2.6 Propellant Feed System

A new propellant refluxing and feed system, shown in Figure 11, was designed and fabricated. This system is a positive displacement device. A piston, driven by a synchronous motor turning a threaded rod, pushes the liquid inside a ground glass tube. The motion of the piston is varied by using a series of synchronous motors. The mass flows, in milligrams/second, are given below:

Motor rpm:	.5	1	2	4	12	30	60	120
Octoil + TNBAP:	.083	.167	.332	.665	1.99	4.99	9.97	19.9
Pure Glycerol:	.106	.211	.423	.846	2.54	6.34	12.7	25.4
Glycerol + NaI:	.114	.229	.457	.915	2.74	6.86	13.7	27.4

This system has been described in Reference 2. In order to avoid the presence of bubbles in the propellant, the system has been designed in such a manner that the propellant is constantly handled in a vacuum. The propellant is stored in a glass container which is heated by an infra-red lamp and is evacuated by a two-inch oil diffusion pump. When needed, the propellant can be gravity fed into the glass tube which is, itself, inside an evacuated pyrex sleeve. This system has operated very satisfactorily. Its only limitation was that accelerating voltages above 10 kilovolts caused a substantial leakage of electric current to take place through the rarefied gas in the plastic hose which connects the pump to the vacuum chamber and to the pyrex sleeve. To permit accurate measurements of the total current supplied into the system by the generator, this limitation was corrected by disconnecting the insulating board on which the pyrex sleeve and the piston advancement mechanism are mounted from the propellant reservoir.

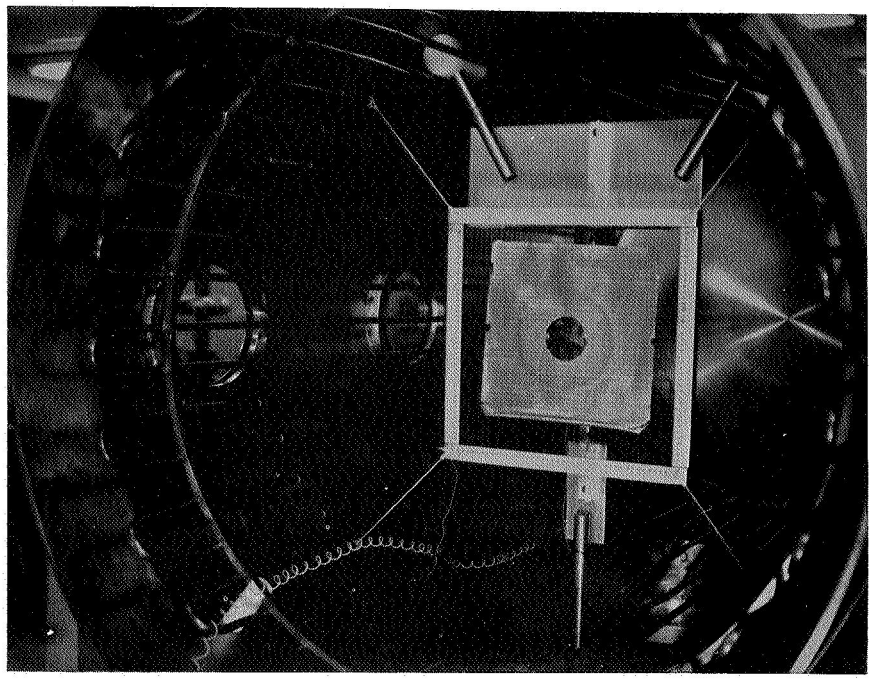

Figure 9. Chamber with Full Beam Target and Screen

Figure 10. Full Beam Target with Balance

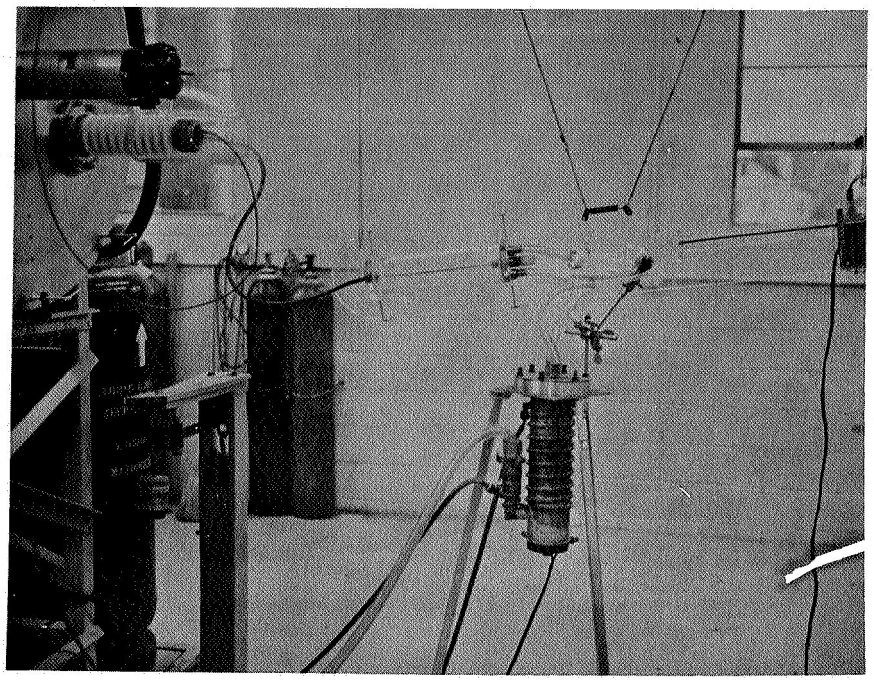

Figure 11. Propellant Refluxing and Feed System. To the left is the high voltage bushing and the magnetic feedthrough.

2.7 Power Supply

The power supply utilized is a constant oblique field electrostatic generator made by Cosmic, Inc. (Reference 4). This generator consists of four 5-inch disks, operating in a pressurized atmosphere of 250 psi. It is capable of 100 kilovolts and two milliamperes. There are two advantages that made an electrostatic power supply such as this more desirable for this type of experiment. First, it has a short circuit current which is only 50 percent higher than the nominal current so that, in addition to being harmless in case of human contact, the damage to equipment inside the vacuum chamber is also considerably reduced. Second, it has practically no internally stored energy so that a spark in the vacuum chamber, originating from say, the edge of the nozzle, will involve only the energy contained the interconnecting cables. This last feature is of some advantage in preventing burning of propellant at the edge of the nozzle.

2.8 Instrumentation

On a separate control console, currents to the following are measured: extractor, screen, collector or target, and the support of the collector or target. The total current from the electrostatic generator is indicated by a meter operating in an insulated housing at the high voltage terminal (Figure 12).

The propellant mass flow is determined by the rate of advancement of the piston in the ground glass cylinder. The voltage is measured on the main control console, but may also be fed to the X-axis on an X-Y plotter for plotting the various currents as a function of the accelerating voltage.

The thrust measuring system deserves a more detailed description. It consists of a Cahn Instrument Company, Model RG Electrobalance and a target assembly. The electrobalance has a maximum sensitivity of 0.5 micrograms and a maximum measurable weight change of 1 gram. It is in two sections, a balance assembly and a control unit. The balance assembly is mounted in the vacuum chamber (Figure 10) and the control console (Figure 13). Weight ranges of 0 to 5, 50, 100, 500 and 1000 milligrams can be selected on the control unit without changing the balance setup. With the exception of transient responses, the balance does not move as weight is applied or removed. A small torque motor compensates for the weight changes.

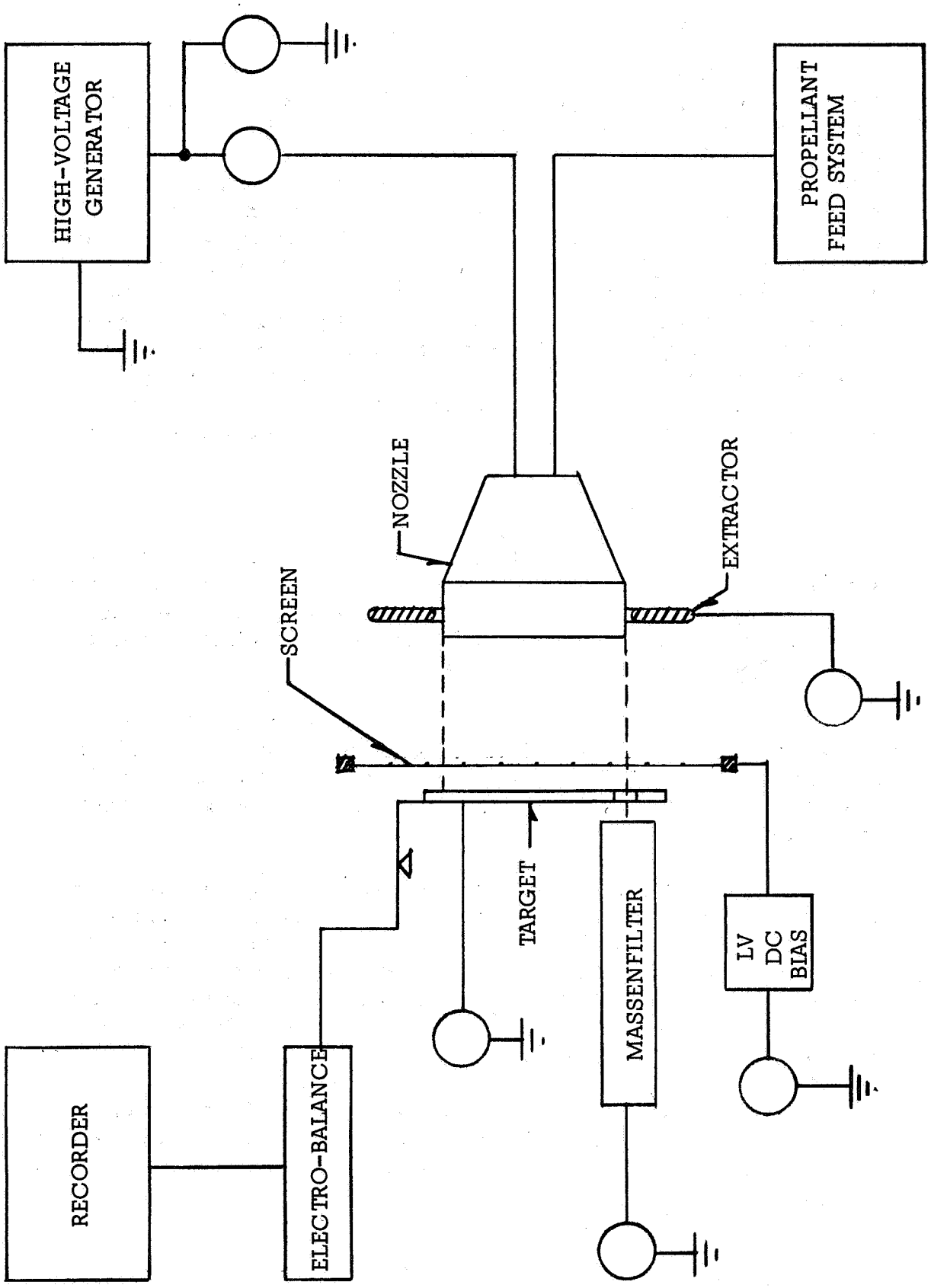

Figure 12. Schematic of Instrumentation

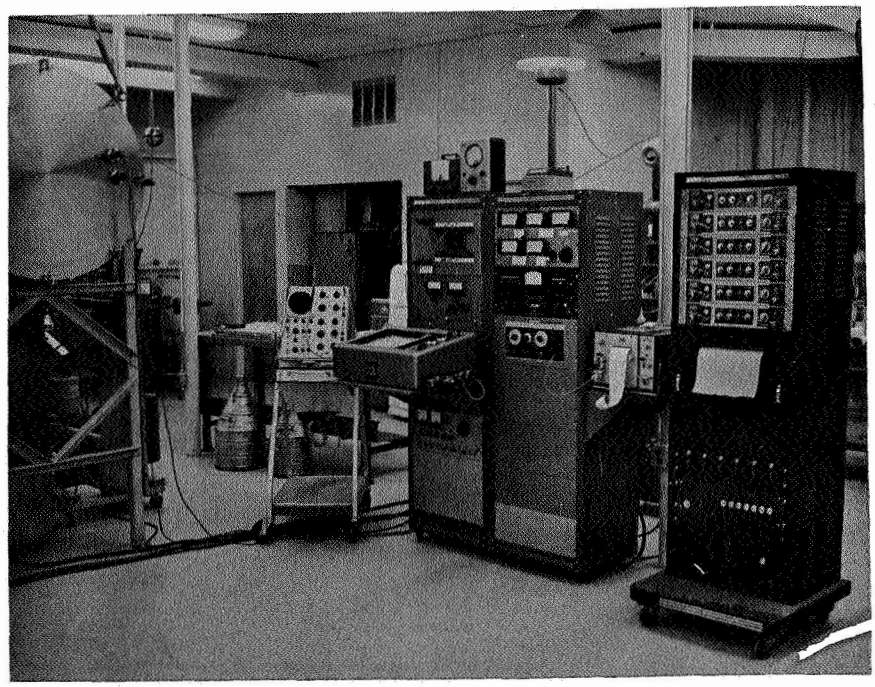

Figure 13. Instrumentation and Control Console. The high voltage terminal of the high voltage generator may be seen behind the control console.

The current supplied to this motor provides the weight indication. This feature readily lends itself to accurate beam thrust measurements since the beam always impacts on the thrust sensing plate, i.e., the target, at the same angle. As previously mentioned, a target assembly that samples a portion of the beam (Figure 8) and a full-beam target assembly (Figures 9 and 14) are available. The small target samples 1/20th of the beam and the full-beam target can be used with a beam up to 8 inches in diameter. Both target assemblies are constructed with equal length lever arms on either side of the fulcrum and the distance to the center of the target is equal to the lever arm length. This permits the thrust or weight change to be read directly from the electrobalance. The bottom edge of the target is curled to form a reservoir to collect any propellant that might otherwise drip off the target so that accurate mass flow readings can be obtained. The plane of the target is centered around and aligned perpendicularly to the axis of the nozzle. The partial beam target is constructed with jeweled bearings at the pivot and the full-beam target is constructed with a knife edge at the pivot. Stability and sensitivity of the balance with both assemblies are good and external clamping is not required.

The high voltage utilized in the system can cause substantial electrostatic forces. In this case, such forces may be of the same magnitude as the forces to be measured. Although this effect could be calibrated and the measurements corrected, it was decided to shield the target from the electrostatic forces by means of a screen. In the case of the collector allowing partial thrust measurement, a grid covers the wedge-shaped hole in the collector. In the case of the full-beam target, a screen larger than the target is placed about $\frac{1}{2}$ inch in front of the latter. In both cases, the screen is biased negatively with respect to the target in order to reflect any possible secondary electrons emitted by the target.

Prior to closing the vacuum chamber for a pump down, the electrobalance is calibrated. Then a precision weight is placed first in the propellant reservoir trough on the target, and then in the target assembly tare bucket to verify the calibration. After the vacuum chamber has reached test pressure, a voltage higher than that to be used during the test is applied to the complete electrobalance thrust measuring system to assure its freedom from electrostatic field force. No change in force or weight should be indicated by the electrobalance. The propellant flow is then initiated.

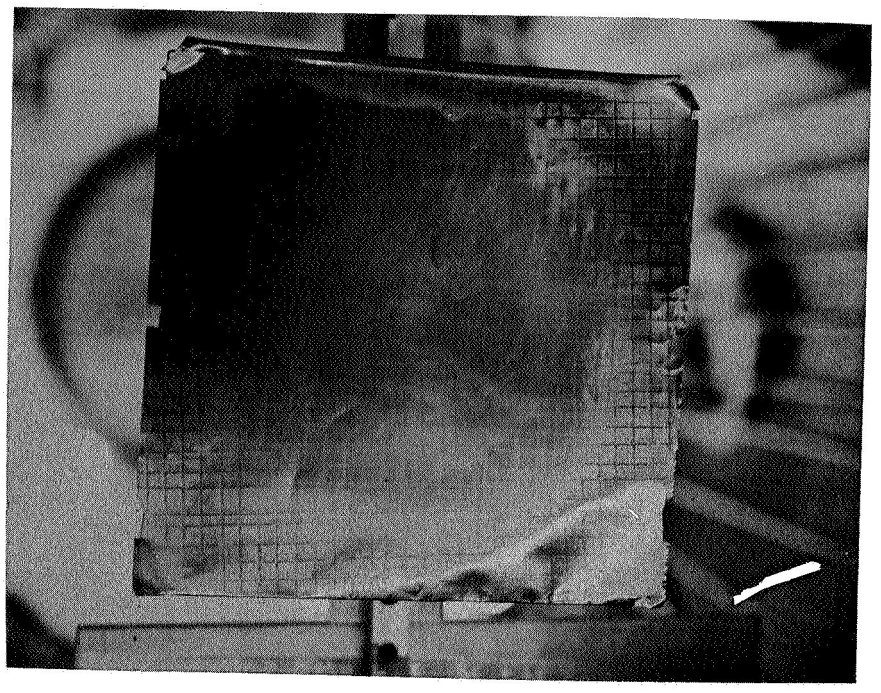

Figure 14. Target and Propellant Pattern

The output of the electrobalance is displayed on a recorder. Since the moment about the suspension point of the weight of the target and of the thrust applied to the target are the same, thrust and mass accumulation on the target (minus evaporation) are read directly from the recorder with no intermediate conversion required. The mass accumulation is the difference between the electrobalance reading for the same value of the accelerating voltage at different times, whereas the beam thrust is measured by the difference between the indications of the electrobalance during the "voltage on" and the "voltage off" operations. The indication of the beam thrust measuring system is fairly sensitive to vibrations, however vibrations coming from the nozzle rotating system are limited in amplitude to the equivalent of 0.1 milligram, and the oscillations due to the mechanical pump are negligible.

A description of the massenfilter, utilized in the program, is found in Reference 3.

2.9 Vacuum Chamber

As pointed out earlier, the liquids utilized in the colloid systems evaporate moderately when placed in a vacuum. Experiments with Octoil, which is itself used as an oil for diffusion pumps, result in fairly little evaporation. However, glycerol undergoes substantial evaporation. As the program described here utilizes mass flows of propellant between 0.5 and 5 milligrams per second, a fairly large vacuum chamber with a high pumping speed was designed.

The vacuum chamber (Figure 15) is five feet long, 32 inches in diameter, and is equipped with five viewing ports. To permit accurate mounting of elements that must be mounted solidly and accurately, such as the spinning nozzle, the two flat ends of the vacuum chamber were designed to act as access doors and are made of 1-inch stainless steel plates machined on both sides. A liquid nitrogen cooling coil occupies the entire length of the chamber. The pump is a 20-inch oil diffusion pump with a rated pumping speed of 16,000 liters per second. The foreline pump is a 15 cubic foot per minute mechanical pump. For easy disassembly, all of the components of the vacuum system and in particular the two end flanges, are suspended from a monorail system.

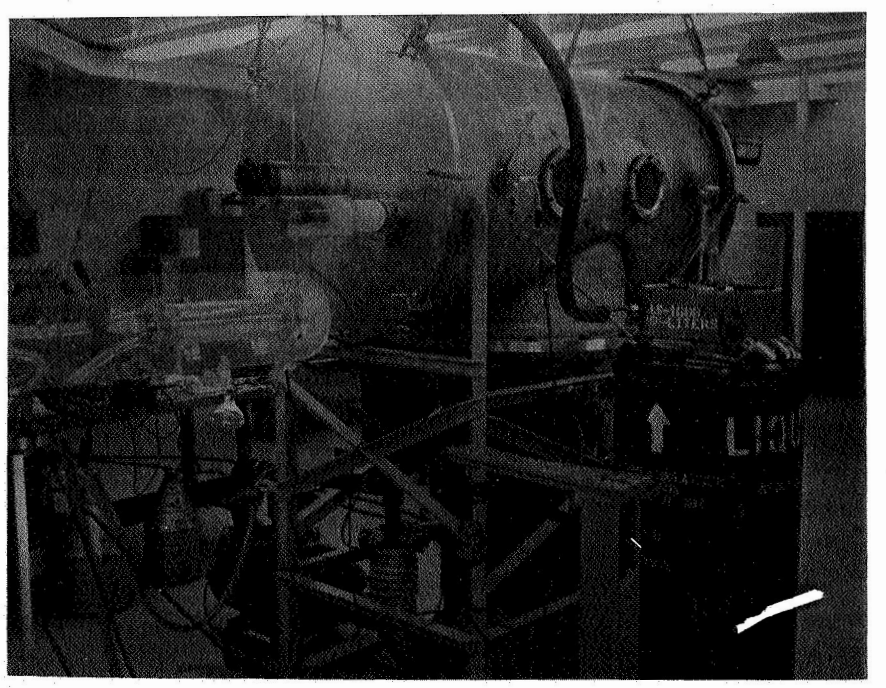

Figure 15. Overall View of Vacuum Chamber

3. TESTS WITH COLLECTOR AND THREE-INCH NOZZLE

In this chapter, we shall relate tests accomplished with a target intercepting only 1/30th of the geometric cross-section of the beam. As explained in Section 2.4, the mass flow calculated from the target measurements are randomly inaccurate. More accurate results will be given in the next section.

3.1 Tests with Octoil

In a previous program (Reference 3), charging had not been possible with Octoil, i.e., with a very clean system the beam current remained at a level corresponding to a charge-to-mass ratio of the order of 1 coulomb/kilogram, even with voltages as high as 80 kilovolts. A number of observations were made in this program and have made it possible to distinguish three modes of operation which are generally obtained sequentially during the same test.

All the tests related below were accomplished with a propellant mass flow of 10^{-6} kilograms/second.

Mode 1. This mode is characterized by voltages up to 90,000 volts and with very little charging. The beam current remains less than one microampere and the pressure remains constant. Even in complete darkness, no glow is visible to a darkness-adapted eye at any point in the vacuum chamber. The propellant is projected towards the collector and accumulates in a circular pattern covering essentially the same position as is the case with the other charging modes. There is no change in the color of the propellant after spraying.

For the purpose of electrostatic propulsion, this mode, which corresponds to charge-to-mass ratios of less than 1 coulomb per kilogram, is not interesting and is considered to be a "no-charging" mode. The fact that the beam is projected onto the collector can be easily explained even though the droplets have "very little" charge-to-mass ratios. At the high voltages used here, the velocity due to electric forces is much larger than the centrifugal velocities. However, the fact that the propellant is not discolored indicates that it has little kinetic energy when hitting the collector. The thrust is not measurable in this mode.

Mode 2. During the operation described above (Mode 1), some beam current may be observed if the voltage is switched on suddenly at a high value (60,000 volts or above). A current of the order of 300 microamperes then appears coincident with a very faint glow around the edge of the nozzle. This current, however, decays to zero and the glow disappears within about 2 or 3 seconds.

After about one hour of operation, with no change in the pressure measured in the chamber, the beam current becomes substantial but varies as a function of voltage in the manner shown in Figure 16. Characteristic of this mode is the fact that the current increases then decreases with an increase in voltage. The difference in pressure between Test 3 and Test 8, shown in Figure 16, is not the only different operating condition, as these two tests were accomplished at several hour intervals with an expenditure of a substantial quantity of propellant and thus, other parameters of the system may have been changed.

In general, during one test the pressure varies in the same direction as the current, as shown in Figure 16, first increasing then decreasing with voltage.

Mode 3. Figure 17 shows a typical current versus voltage curve obtained after several hours of operation with the voltage having been turned off a number of times to obtain thrust readings. During this test, three measurements of charge-to-mass ratio, q/m, and thrust were accomplished.

At 50 KV, q/m = 600 coulombs/kilogram. The thrust measurements were not accurate enough to permit accurate calculations of the efficiency which appeared to be about 0.8, however.

At 55 KV, q/m = 770	Efficiency = 0.56
At 60 KV, q/m = 920	Efficiency = 0.30

After the test during which the data for Figure 17 had been accumulated, the propellant flow was stopped. A new curve obtained (Figure 18) fifteen minutes later. The voltage was then left on at about 76 KV and Figure 18 shows the current decaying slowly as the propellant stored in the nozzle is being expelled. After complete exhaustion of propellant, the current went back to zero. The entire cycle took about one-half hour. This substantial "inertia" of the 3-inch nozzle was one of the reasons for building the 1.7-inch

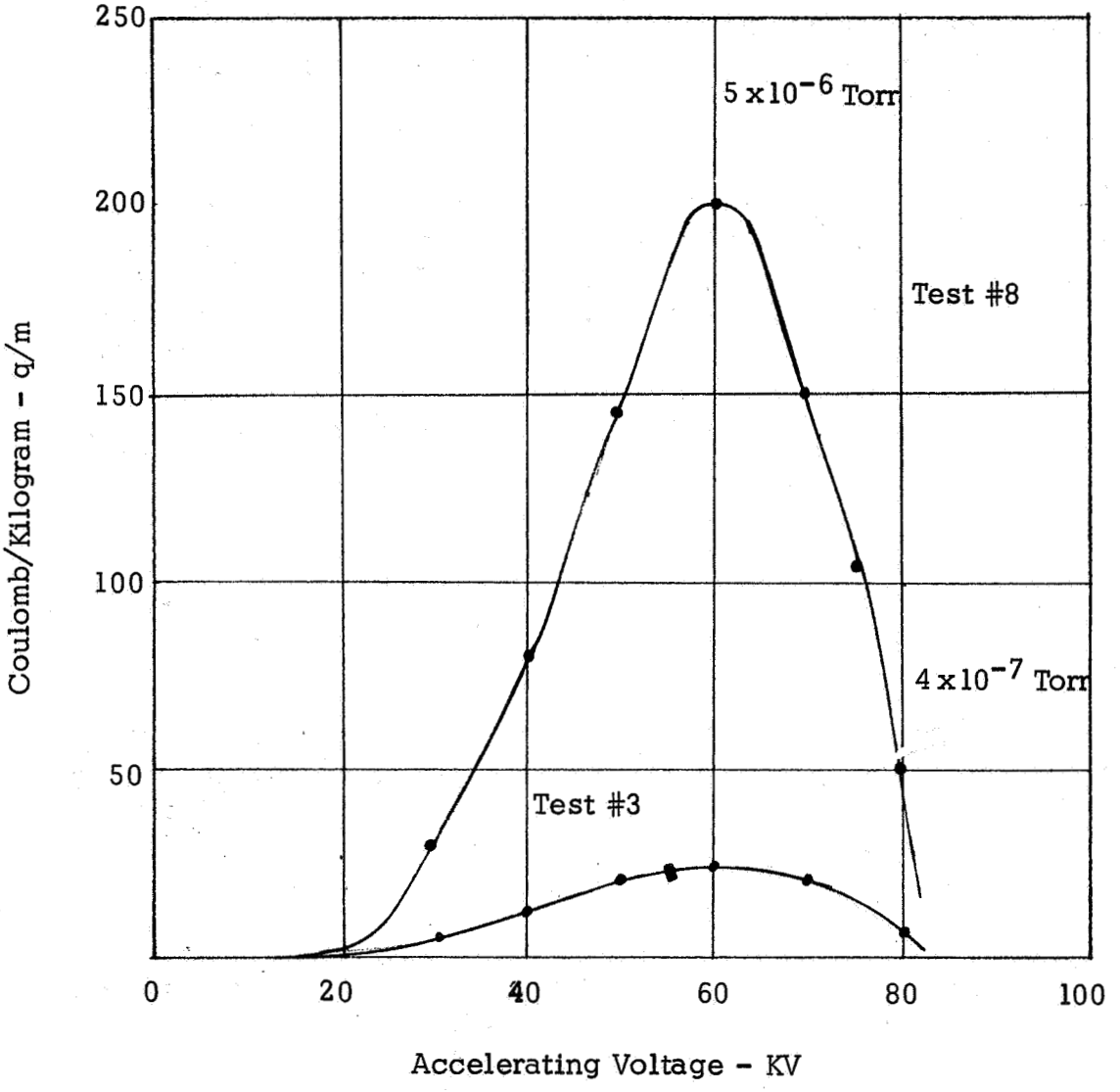

Figure 16. Typical Mode 2 Operation with Octoil.

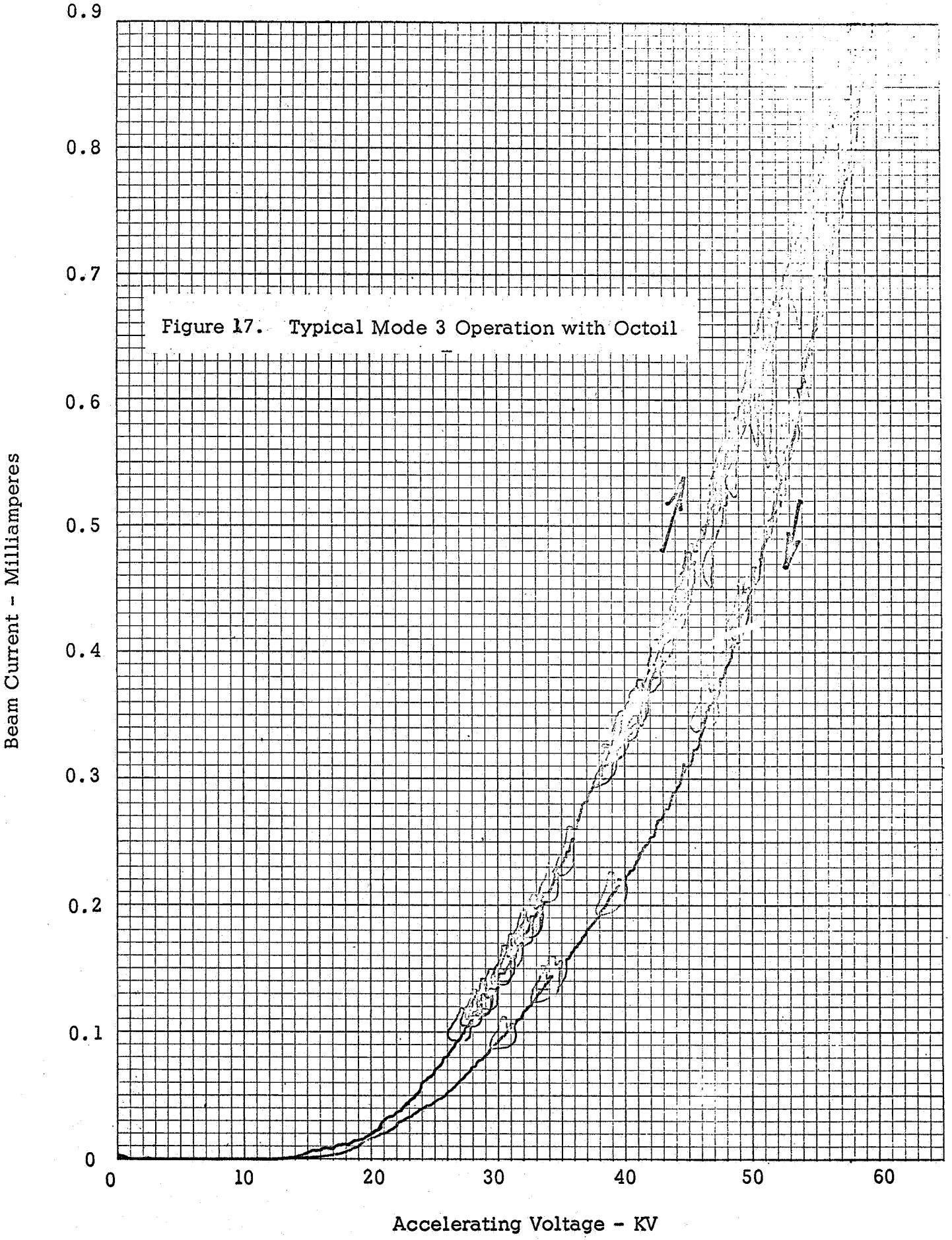

Figure 17. Typical Mode 3 Operation with Octoil

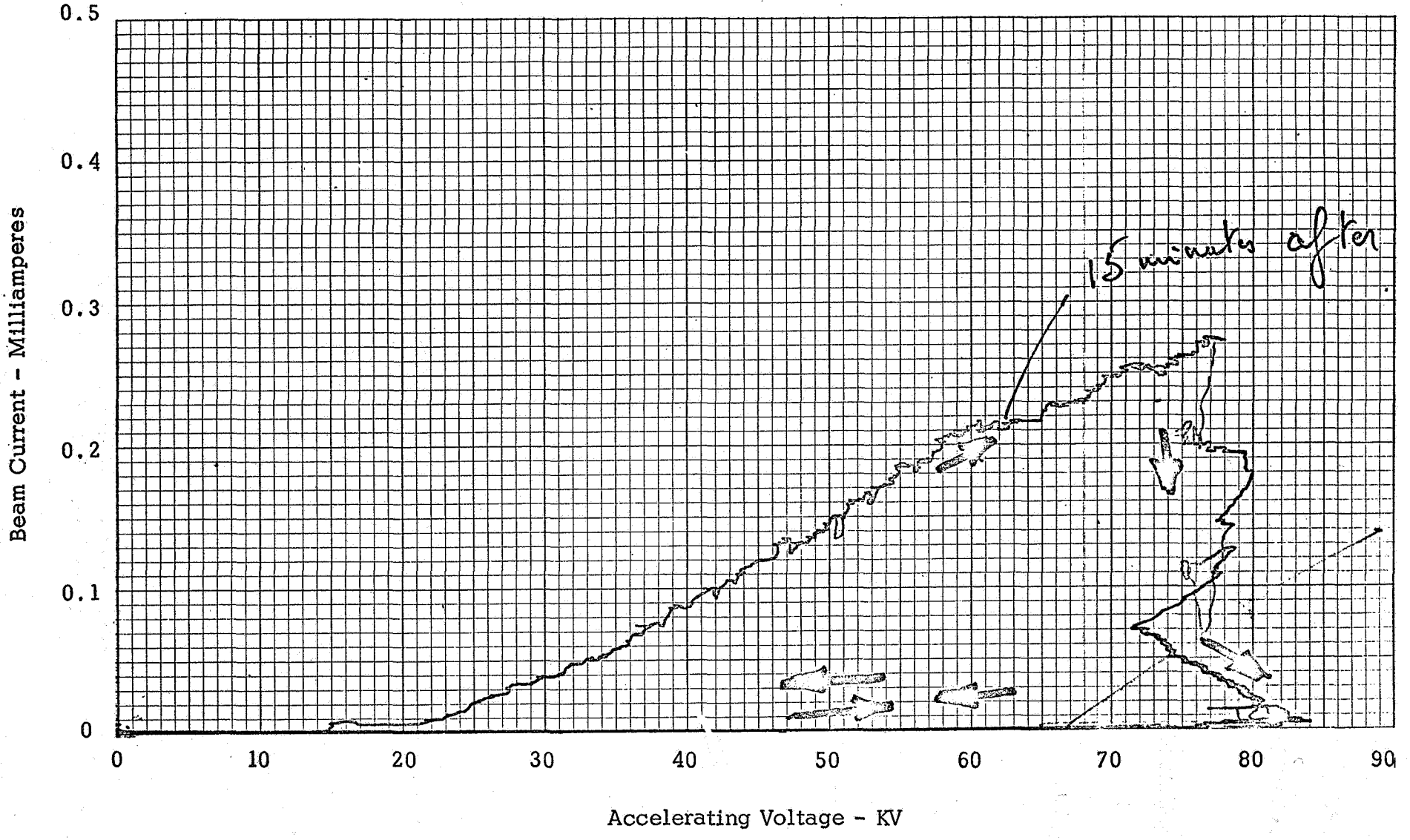

Figure 18. Mode 3 Operation after Propellant Feed System was Shut Off.

nozzle with as little storage of the propellant as possible. This test was performed to make certain that the corona discharge that might be present is associated with the flow of propellant. Other experimenters, in particular Hinrichs (Reference 5), had found that a corona discharge would persist after the propellant flow had been turned off.

The titanium target which had been utilized during this test was removed (Figure 8). It showed considerable erosion, whereas in earlier experiments where the charge-to-mass ratio was limited to 200 coulomb/kilogram, the target itself was not eroded but was covered with a layer of viscous, dark brownish Octoil.

No satisfactory explanation has been found for these three modes. The most plausible explanation for the fact that there is no charging in Mode 1 is due to Dr. A. W. Bright and invokes the double layer mechanism in the following fashion. At all liquid-gas or liquid-vacuum interfaces, there exists an electrical double layer. The electric field due to the double layer neutralizes that due to the potential of the nozzle with respect to the extractor. This phenomenon will be further discussed later in this report.

3.2 Tests with Glycerol

Solutions of glycerol plus sodium iodide were mixed, refluxed, and kept constantly under vacuum in-between the tests. In order to increase the ability of the liquid to wet the nozzle, Calgonite was added although the beneficial effect of the latter could not be ascertained.

A screen was installed in front of the collector and biased sufficiently to repel secondary electrons, if any. With a bias voltage of 200 volts, the following data was obtained:

Voltage	18.5 KV
Target Current	3.8 microamperes
Target Mass Flow	.0012 milligrams/second
Thrust	.92 milligrams

resulting in:

Average $q/m = 3,160$ and $\eta = .46$

With a bias voltage of 27.5 volts, the following measurements were made:

	Run A	Run B	Run C
Voltage	20	20	21
Target Current	4.5	4	3.8
Target Mass Flow	.0012	.0012	.0012
Thrust	1.2	1.2	1.3
Average q/m	2750	3350	3160
Efficiency	.59	.68	.82

All the above data is based on measurement of mass flow accumulated on the target, and tests reported later have shown that this results in seriously underestimated mass flows in the case of glycerol. The charge-to-mass ratio and the efficiencies given above are therefore overestimated.

In all tests with glycerol, a glow was always visible for a darkness-accustomed eye.

The evaporation of glycerol was investigated. Five days of exposure to vacuum were required to obtain complete evaporation of 20 drops of glycerol on a 2-square-centimeter area. This would indicate that during one test (3 hours), evaporation from the liquid already on target cannot be substantial. It must be born in mind that the kinetic energy of the particles is very high at the time of impact so that it is quite possible that substantial evaporation takes place making it difficult to measure mass flow by weighing the target. One can then contemplate utilization of the measurement of the total mass flow injected into the system, and take the portion of this mass flow proportional to the portion of the beam intercepted by the target. Even though the beam appears from visual inspection of its trace on the collector to by symmetrical, attempts to calculate the mass flow on the target by this method have always failed. In view of this uncertainty, it appeared essential to obtain thrust measurement on the total beam so that the mass flow, as measured on the propellant feed system, could be utilized in accurate efficiency calculations.

4. TESTS WITH FULL-BEAM TARGET AND 1.7-INCH NOZZLE

The nozzle used in these tests was a 1.7-inch outside diameter stainless stell nozzle with a one-degree internal slope (Figure 3). An extractor with an internal diameter of 1.8 inches, located 0.10 inches behind the edge of the nozzle, was used. The test procedure followed was the following: The vacuum chamber and the propellant auxiliary vacuum chamber are pumped until the pressure has remained below 2×10^{-6} Torr for several hours. The propellant supply tube is loaded, the auxiliary vacuum chamber is sealed and the auxiliary vacuum pump disconnected from the system. With the nozzle slowly rotating (about 1000 rpm), the system is "conditioned" by applying a voltage to the nozzle which is increased until the first sign of breakdown, which usually occurred between 20 to 30 KV. The voltage is then reduced about 5 KV and left on for half an hour at which time the voltage is increased in 5 KV steps for half-hour intervals until a 35 to 40 KV level is reached. The system is allowed to remain at this level for at least half an hour for final conditioning. At this time, the thrust measuring system is checked to be sure it is not being influenced by any electrostatic forces by varying the voltage from 0 to 30 KV and observing the output of the electrobalance on the recorder for any apparent weight changes; there should be none. The voltage is then reduced to about 10 KV and the propellant flow initiated. When a steady propellant flow is established, the test is started.

The time required for the flow of propellant to be started is about 15 minutes with the 1 rpm feed motor. The beam current then is increased gradually for another 15 minutes and the collection of propellant on the target can be observed. In all these tests, glycerol plus sodium iodide was utilized as a propellant and it was found to behave similarly to Octoil in Mode 1, described earlier, but only for a brief period. Cycling of the voltage on and off, as required for thrust measurement, resulted initially in an increase of both thrust and current until a steady operation was reached. Typical results are shown in Table I. Each run lasted between 1 hour and 8 hours. The duration of a test does not seem to change operating conditions very much and does not result, in particular, in a change in pressure.

The thrust measurements with this full-beam target are accomplished with precision as can be seen from a typical recording, shown in Figure 19. Accuracy of these thrust measurements then follows from the calibration of the Cahn balance and the fact that the total beam is intercepted by the target. The calculation of efficiency is accomplished by the nomogram (Figure 20).

Run Number	Mass Flow $\dot{m}$ (mg/sec)	Thrust F (mg)	Current I (μa)	Voltage V (KV)	Efficiency η	Charge-to-Mass Ratio q/m coul/kg	Screen Bias Voltage V
1	.25	40	20	30	.51	80	
2	.25	54	60	40	.23	240	
3	.25	75	500	26	.10	2000	
4	.25	80	40	34	.88	160	40
5	.25	60	60	26	.42	240	40
6	.25	60	200	26	.16	400	
7	.25	36	200	20	.07	400	
8	.25	40	170	27	.08	680	
9	.25	85	90	26	.46	280	
10	.5	20	6	20	.31	12	
11	.5	75	50	26	.43	100	
12	.5	85	90	24	.31	180	
13	.5	90	130	24	.25	460	
14	.5	170	500	21	.26	1000	
15	.5	90	230	22	.14	460	
16	.5	70	95	27	.18	190	
17	.5	150	400	21	.25	800	
18	.5	20	2.5	20	.80	5	
19	.5	150	120	21	.17	240	

Table I: Summary of Test Data with Full Beam Target

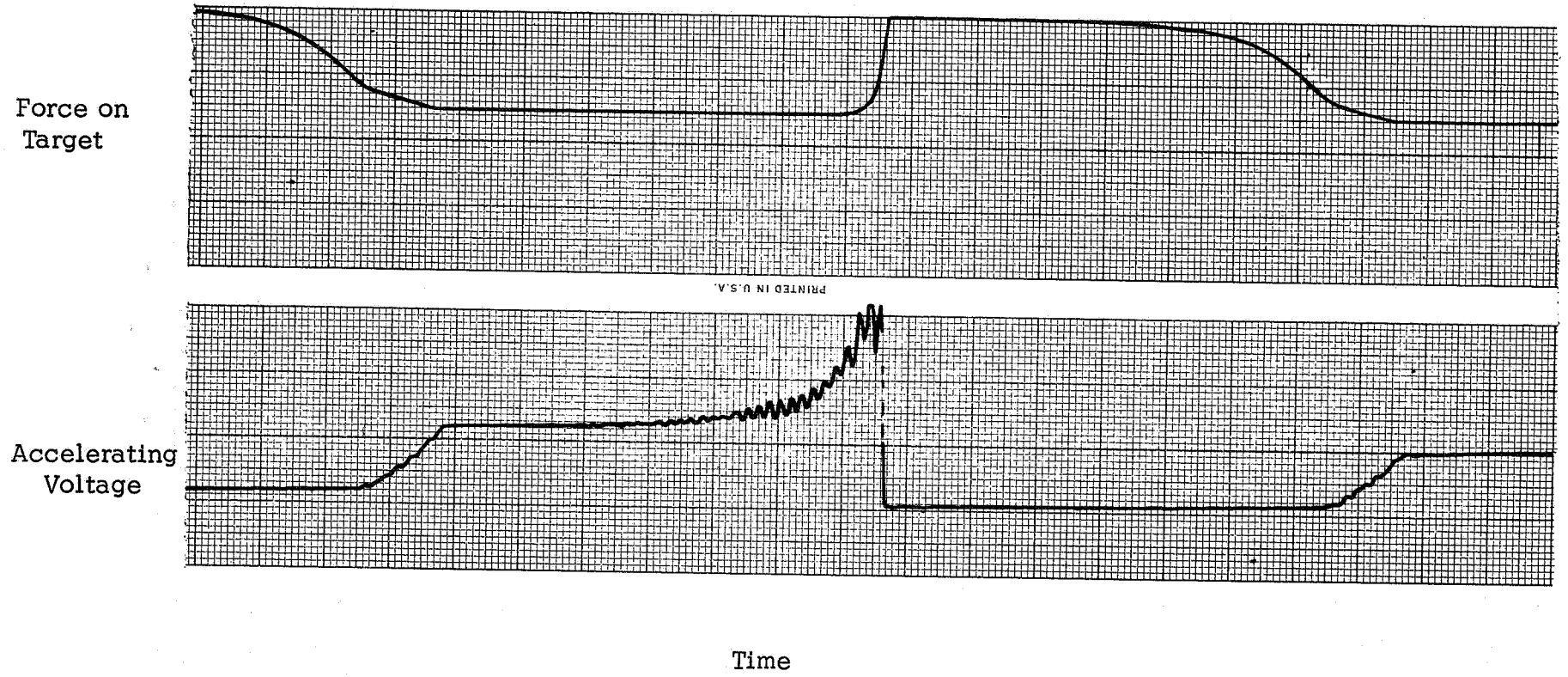

Figure 19. Thrust Recording with Simultaneous Acceleration Voltage Record.

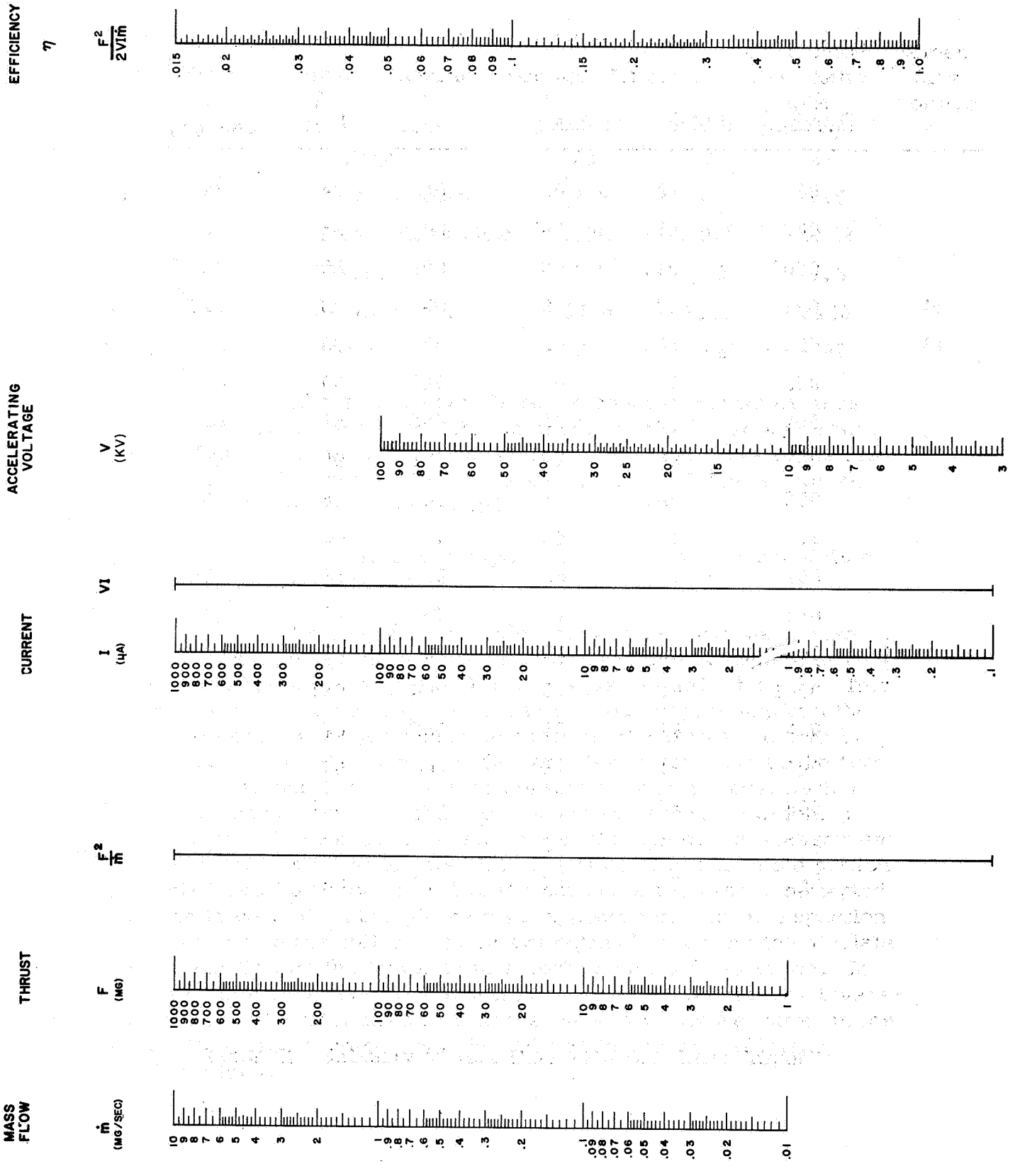

Figure 20. Nomogram for Calculations of Efficiency

A typical beam current versus voltage curve as obtained by the X-Y plotter is shown in Figure 21.

During the tests accomplished in darkness, it was noticed that two zones were flowing in the space between the nozzle and the target. Thus, one could observe a cone of light essentially extending the nozzle and a small beam of light along the axis of symmetry striking the collector in a circle approximately 0.7 cm in radius. It had been suggested by Professor Loeb that an experiment be accomplished to determine if the central beam contained a substantial current. The arrangement shown in Figure 9 was then utilized, another "central target" being placed so as to intercept the beam passing through the hole in the first target. The results obtained were as follows with the voltage in kilovolts, the current in microamperes and the thrust in milligrams:

Voltage	Target Current	Thrust	Efficiency
18	36	45	.38
22	220	90	.21
20	77	60	.33
24	420	125	.18

The mass flow was 0.41 milligram/second. There was a negligible current (less than 1 microampere) on the central target. Mass filter readings were also taken (Figure 22) through a window in the full-beam target. The quadrupole assembly was aligned optically along the beam. The results obtained were difficult to interpret as current readings on the quadrupole varied by a factor of 2 with time during one experiment. It must be borne in mind that the aperture of the quadrupole has a very small cross-section and is therefore sensitive to sweeping of the beam due to very small voltage instabilities. It was felt that the thrust measurements were a much better method of obtaining efficiency than the integration of quadrupole mass filter data. For this reason, the efficiencies shown above were calculated from thrust measurements.

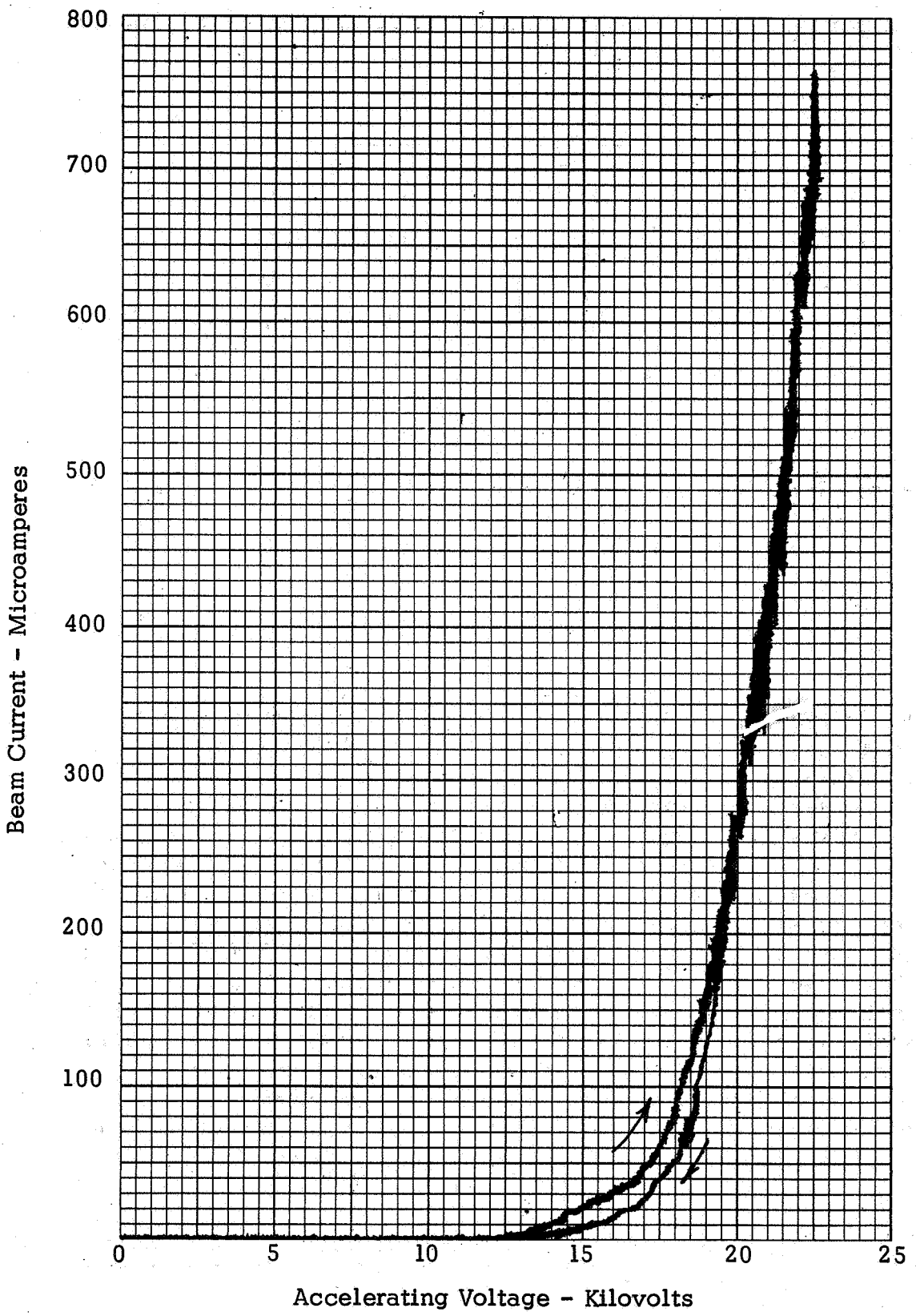

Figure 21. Beam Current vs Accelerating Voltage

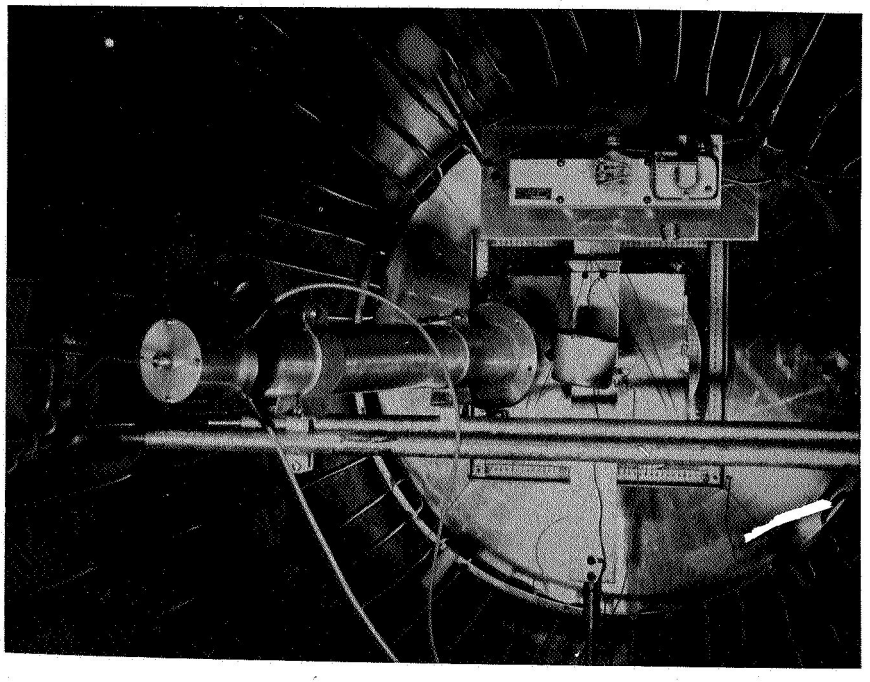

Figure 22. View of Massenfilter Mounted Behind the Full-Size Target.

5. DISCUSSION OF CHARGING MECHANISMS

In this section, we shall examine the mechanism whereby electric charges are transferred from the nozzle to the colloid beam of charged particles. Following the movement of the electric charges, the problems to be examined are the transfer of electric charges from the nozzle to the outer edge of the liquid covering the nozzle, the transfer of electric charges from this outer edge onto the droplets, and finally, the distribution of electric charge among the droplets which can then be looked upon as a flow of a finely-divided liquid in which each droplet has a certain size and a certain charge-to-mass ratio. For convenience in this report, we shall talk about each of these aspects of the problem in the reverse sequence. We shall first examine the distribution of size versus charge-to-mass ratio of the droplets. Taking a droplet or system of droplets free in space, one can see that the forces present are the electrostatic pressure which is exerted outward with respect to each droplet and tends to break it into several sub-droplets, and the surface tension forces which tend to maintain the droplet in a spherical shape. The theoretical development which is subject to the least controversy is the so-called Rayleigh criterion for determining the maximum size of the particles as a function of their charge-to-mass ratio (Reference 6). In brief, this criterion says that the maximum charge of the droplet is the one for which the electrostatic forces, which tend to make the droplet explode into several smaller droplets, is exactly equal to the force due to the surface tension. Rayleigh demonstrates that any charge below this maximum corresponds to a stable state, whereas a droplet having a higher charge will necessarily be unstable. The criterion of Vonnegut and Neubauer (Reference 7) is different in that it considers the problem of how a given total charge equally dispersed in a given total mass in a system of droplets will determine droplet size. The consideration here is that the energy of the system should be a minimum for the equilibrium to take place. The calculation accomplished by Vonnegut and Neubauer gives a size of droplet that is smaller than that obtained by the Rayleigh criterion. In fact, a "Vonnegut droplet" would be that which is obtained if a "Rayleigh droplet" were to be split in four equal smaller droplets. How do these criterion help us determine what is the size of the droplets in a colloid beam? In order to answer this question, we should know what the charging mechanism is, as the calculation of Lord Rayleigh would be valid in the case of a droplet which is charged say by electron attachment to a level which happens to be just below that at which it explodes. On the other hand, the calculations of

Vonnegut and Neubauer assume that the droplet cannot only split, but also can coalesce - a very unlikely situation indeed in a colloid beam. As will be seen later on, the charging mechanism involved here is fairly complex and is likely to involve charge attachment performed in a nonuniform electric field. Thus, what can be said with certainty is that the Rayleigh criterion constitutes an upper limit for the charge-to-mass ratio of particles of a given size. Furthermore, in view of the fact that the minimum energy consideration does result in a size not too different than that obtained by the Rayleigh criterion, it appears that the latter can be considered as a good first approximation of the actual droplet size.

The second aspect of the charging problem which can be examined only qualitatively is that of the mechanism whereby electric charges are transferred onto the droplets themselves. At the initiation of the program, it was felt that the charge was obtained by an induction mechanism. Whenever a conductor is submitted to an electric field, a charge density is established on the surface of the conductor which is proportional to the electric field outside the conductor. If the liquid covering the nozzle and the edge of the nozzle can be considered to be a perfect conductor, a charge density will then be established on the liquid surface and when a portion of the liquid is separated from the nozzle, this portion of the liquid and its electric charge are removed instantaneously. Experimental results of the colloid nozzle show that this theory is an oversimplification to say the least. First it was found that with a good vacuum and a clean nozzle there was no charging of liquid metals. Then, it was discovered that charging occurs only when a glow can be seen at the edge of the nozzle. As the system was perfected making it possible to operate with better prepared surfaces and a higher vacuum regardless of the evaporation in the vacuum chamber, the same phenomenon occurred with Octoil and finally, but less markedly, with glycerol. With Octoil, the additional fact was discovered that when operating at relatively high voltages (of the order of 50 kilovolts) the spraying of the colloid beam had the effect of decreasing the pressure inside the vacuum chamber. This phenomenon can be explained by the fact that the liquid traps the gases as it collects on the collector. In this respect, the operation can be compared to that of a titanium evaporator pump in which titanium, being projected against the relatively cold walls of the evaporator, traps the molecules of gases without combining with them. There is no satisfactory theory to explain this phase of the charging mechanism. The most plausible explanation is the one which was advanced by Professor Leonard Loeb, a consultant to the program, and which invokes the corona mechanism. At the pressure involved, the main free path

of the molecules of the residual gas is large as compared to the distances between the extractor and the nozzle or as compared to the area which can be observed to glow. The corona discharge is therefore maintained by decomposition of a part of the liquid propellant itself and not by ions of the ambient gases. Thus, one can consider as a possibility that droplets are being formed at the edge of the nozzle and thereafter bombarded by ions resulting from the partial decomposition of the propellant in the glow area around the edge of the nozzle. If this is truly the charge mechanism, it is well to notice that there is nothing that would make such a charging mechanism less capable than others to produce charge-to-mass ratios in the desired range, or high efficiency. Generally, charging by bombardment or attachment is assumed to result in poor efficiency, however, in this case both the droplets and the ions which are going to attach themselves to the droplets originate from the same area so that the chances of an ion being captured by a droplet are much greater than would be the case if a stream of droplets were bombarded by a source not related to the stream.

Finally, we must now examine the mechanism whereby the electric charges are transferred from the middle of the nozzle to the outer surface of the liquid. In other words, the problem is that of conductivity through the liquid. It should be recognized at first that the conducticity through organic liquids is due mostly to the presence of ionic impurities. This conductivity, however, is also responsible for another effect which is the presence of electric double layers on the boundary surfaces of the liquid. The importance of these double layers has been recognized in the recent work accomplished in the petroleum industry (Reference 8). Electrostatic charging due to double layers can occur when liquids are being transferred. It is only recently that it has been realized that conductivity in liquids, previously thought to represent intrinsic processes in the liquid, were in fact due to impurities. However, most of the work in this field has been directed towards limiting conductivity. The work of Wineland and Hunter (Reference 9) is valuable as the influence of the double layer is postulated and discussed in a configuration adaptable to an electrostatic thrustor. The conductivity which is of interest here is the conductivity of a liquid submitted to a very intense electric field for a very brief period of time and it should be pointed out that such conductivity is very different from that normally measured in laboratories under steady conditions for widely separated electrodes at low voltages.

An illustration of the difference between the various definitions of conductivity is given by Hogan (Reference 10) who obtained, by mixing Cab-O-Sil with Octoil, results comparable to those obtained by increasing the conductivity of Octoil. However, a mixture of Cab-O-Sil and Octoil does not show an increase in conductivity over pure Octoil when measured with a low voltage tester.

It is well to recognize that electrical double layer phenomena generally involve electric charge density of relatively low values. Thus, in the natural atomization of liquids by, say, a rotating nozzle in the absence of an external field, the droplet may have a surface charge of the order of 0.3 to 1 coulomb/meter^2. For droplets of millimeter size, this corresponds to about 1 coulomb/kilogram. For droplets of submicron size, it would correspond to several thousand coulombs/kilogram. The fact to bear in mind here is that the double layer charging effect can be utilized to explain the charge or lack of charge on a droplet formed by other means, but cannot by itself cause atomization into droplets of the desired size.

A theoretical analysis of the overall charging mechanism has been attempted on the assumption that the charge per unit area of droplets is proportional to the electric field at the edge of the nozzle. This is the case in induction charging mechanisms and may also be the case with other charging mechanisms. And because it might be of general applicability, it will be summarized here in its application to trends, i.e., the variation of the charge-to-mass ratio as a function of the operating parameters.

The method pursued has consisted in analyzing two extreme cases for the beam: a weak space charge case and a strong space charge case and two assumptions for the charging mechanism: one in which the droplets have a size comparable to the film thickness (extraction mode of charging) and one in which the particle size is dictated by a Rayleigh-like stability criterion (Reference 6). We shall only indicate here the results of this analysis which gives the performance parameters as a function of the following controllable elements:

$\dot{m}$ = Mass flow
V = Voltage
L = Characteristic length of accelerating system
r = Radius of nozzle
ω = Rotating speed

ν = Kinematic viscosity of propellant
γ = Surface tension of propellant
ρ = Mass density of propellant
σ = Conductivity of propellant

Only the value of the charge-to-mass ratio, q/m, will be given, the other quantities such as thrust, current, etc., can be derived by their functional relation to q/m.

In the strong space charge case, the relation is (Reference 2):

$$\frac{q}{m} = V^3 L^{-4} \dot{m}^{-4/3} \omega^{-4/3} r^{2/3} \nu^{2/3} \rho^{-2/3}$$

In the weak space charge case, the relation is different for the extraction mode and the disintegration mode and may be written:

$$\frac{q}{m} = V L^{-1} \dot{m}^{-1/3} \omega^{2/3} r^{2/3} \nu^{-1/3} \rho^{-2/3} \left[1 - \exp\left(\frac{\sigma \tau}{\epsilon}\right)\right]$$

in the extraction mode and

$$\frac{q}{m} = V^3 L^{-3} \rho^{-1} \nu^{-1} \left[1 - \exp\left(-\frac{\sigma \tau}{\epsilon}\right)\right]^2$$

in the disintegration mode, τ being a characteristic time available for charging the droplets.

To date, some of the data obtained has been in agreement with the disintegration mode of the weak space charge case.

As the data obtained cannot be made to agree with one theory entirely, let us analyze qualitatively the conclusions which can be drawn from the data and can have some influence on the charging mechanism.

1. The charge-to-mass ratio increases with conductivity for a given liquid. Thus for Octoil, for which systematic experiments have been performed varying the conductivity, the data is not incompatible with the exponential law given above for the variation of the charge-to-mass ratio with conductivity.

2. Charging of the propellant to a significant value (larger than 1 coulomb/kilogram) is always accompanied by a glow visible to a darkness-accustomed eye inside the vacuum chamber. This glow concentrates on the edge of the nozzle and does not necessarily fill the entire space between the nozzle and the extractor or between the nozzle and the collector.

APPENDIX

TESTS WITH A SINGLE NEEDLE SOURCE OF COLLOID

In order to compare operation of the spinning nozzle with that of capillary sources, several needles have been operated in the 3 x 5 foot vacuum chamber with the pressure in the middle 10^{-7} Torr range. The needles used had a bore of 0.004 inch and an outside diameter of 0.008 inch. Thrust measurements up to 0.9 milligram and beam currents up to 8 microamperes on the target and 12 microamperes on the collector (the target intercepts about one-half the beam) have been observed. Reliable mass flow measurements have not been possible

These tests have shown operation of one needle is not qualitatively different from that of a spinning nozzle. No calculation of efficiency was possible, however.

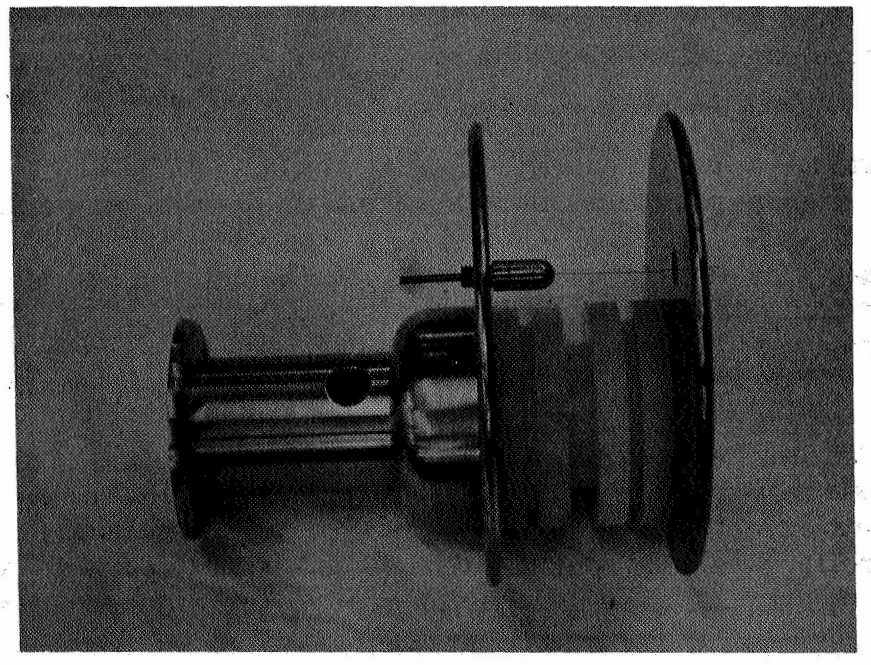

Figure A1. Single Needle.

REFERENCES

1. William R. Mickelsen and Harold R. Kaufman, NASA TN D-2172, "Status of Electrostatic Thrustors for Space Propulsion", May 1964.

2. D. Gignoux, H. F. Anton, J. J. Shea and R. M. Moriarty, "Further Development of a Charged Liquid Colloid Source for Electrostatic Propulsion". NASA CR-54642 (Cosmic, Inc. Report No. 106), October 1965.

3. D. Gignoux, H. F. Anton, and J. J. Shea, "Development of a Charged Colloid Source for Electrostatic Propulsion". NASA CR-54176 (Cosmic, Inc. Report No. 82), October 1964.

4. D. Gignoux, "Electrostatic Generators in Space Power Systems". J. of Spacecraft and Rockets, Vol. 3, No. 12, pp. 1803-1805, December 1966.

5. C. K. Hinrichs, "An Investigation of a Charged Colloid Propulsion System", Aerojet-General Report AN-683.

6. Lord Rayleigh, "The Equilibrium of a Liquid Conducting Mass" Philosophical Magazine, 14, 184, (1882).

7. B. Vonnegut and R. L. Neubauer, J. Colloid Sci. 7, 616, (1952).

8. Klinkenberg and Van der Minne, "Electrostatics in the Petroleum Industry" (New York, Elsevier, 1958).

9. S. H. Wineland, W. C. Burson, and R. E. Hunter, "The Electrohydrodynamic Generation of Charged Droplet Beams", Technical Report AFAPL-TR-66-72, Air Force Aero Propulsion Laboratory, Wright-Patterson Air Force Base, Ohio, August 1966.

10. J. J. Hogan, "Parameters Influencing the Charge-to-mass Ratio of Electrically Sprayed Liquid Particles", Charged Particle Research Laboratory Report No. CPRL-2-63, December 1963.

FINAL REPORT DISTRIBUTION LIST

CONTRACT NAS3-7924

	Addressee	Number of Copies
1.	National Aeronautics and Space Administration Washington, D. C. 20546 Attention: RNT/James Lazar	1
2.	NASA-Lewis Research Center 21000 Brookpark Road Cleveland, Ohio 44135 Attention: Spacecraft Technology Procurement Section (M.S. 3-19)	1
3.	NASA-Lewis Research Center 21000 Brookpark Road Cleveland, Ohio 44135 Attention: Technology Utilization Office (M.S. 3-19)	1
4.	NASA-Lewis Research Center 21000 Brookpark Road Cleveland, Ohio 44135 Attention: Technical Information Division (M.S. 5-5)	1
5.	NASA-Lewis Research Center 21000 Brookpark Road Cleveland, Ohio 44135 Attention: Library (M.S. 60-3)	2
6.	NASA-Lewis Research Center 21000 Brookpark Road Cleveland, Ohio 44135 Attention: Spacecraft Technology Division C. C. Conger (M.S. 54-1)	1
7.	NASA-Lewis Research Center 21000 Brookpark Road Cleveland, Ohio 44135 Attention: Spacecraft Technology Division E. W. Otto (M.S. 54-1)	1

	Addressee	Number of Copies
8.	NASA-Lewis Research Center 21000 Brookpark Road Cleveland, Ohio 44135 Attention: Spacecraft Technology Division H. R. Hunczak (M.S. 54-3)	1
9.	NASA-Lewis Research Center 21000 Brookpark Road Cleveland, Ohio 44135 Attention: Spacecraft Technology Division P. Ramins (M.S. 54-3)	2
10.	NASA-Lewis Research Center 21000 Brookpark Road Cleveland, Ohio 44135 Attention: Electric Propulsion Laboratory W. Moeckel (M.S. 301-1)	1
11.	NASA-Lewis Research Center 21000 Brookpark Road Cleveland, Ohio 44135 Attention: Electric Propulsion Laboratory H. R. Kaufman (M.S. 301-1)	1
12.	NASA-Lewis Research Center 21000 Brookpark Road Cleveland, Ohio 44135 Attention: Electric Propulsion Laboratory E. Richley (M.S. 301-1)	1
13.	NASA-Lewis Research Center 21000 Brookpark Road Cleveland, Ohio 44135 Attention: Electric Propulsion Laboratory C. T. Norgren (M.S. 301-1)	1
14.	NASA-Lewis Research Center 21000 Brookpark Road Cleveland, Ohio 44135 Attention: Report Control Office (M.S. 5-5)	1

	Addressee	Number of Copies
15.	NASA Scientific and Technical Information Facility P. O. Box 33 College Park, Maryland 20740 Attention: NASA Representative RQT-2448	6
16.	NASA-Marshall Space Flight Center Huntsville, Alabama 35812 Attention: Ernest Stuhlinger (M-RP-DIR)	1
17.	AFWL Kirtland AFB, New Mexico 87417 Attention: WLPC/Capt. C. F. Ellis	1
18.	Aerospace Corporation P. O. Box 95085 Los Angeles, California 90045 Attention: Library/Technical Documents Group	1
19.	Jet Propulsion Laboratory 4800 Oak Grove Drive Pasadena, California 91103 Attention: J. J. Paulson	1
20.	Hughes Research Laboratories 3011 Malibu Canyon Road Malibu, California 90265 Attention: Dr. Ron Knechtli	1
21.	Electro-Optical Systems, Inc. 300 North Halstead Street Pasadena, California 91107 Attention: A. T. Forrester	1
22.	Ion Physics Corporation South Bedford Street Burlington, Massachusetts 02103 Attention: Sam Nablo	1

	Addressee	Number of Copies
23.	TRW Inc. TRW Systems Group One Space Park Redondo Beach, California 90278 Attention: D. B. Langmuir	1
24.	Westinghous Astronuclear Laboratories Electric Propulsion Laboratory Pittsburgh, Pennsylvania 15234 Attention: H. W. Szymanowski, Manager	1
25.	NASA-Ames Research Center Moffett Field, California 94035 Attention: Library	1
26.	Aerojet-General Nucleonic Division San Ramon, California 94583 Attention: J. S. Luce	1
27.	NASA-Langley Research Center Langley Field Station Hampton, Virginia 23365 Attention: Technical Library	1
28.	Colorado State University Fort Collins, Colorado 80521 Attention: L. Baldwin	1
29.	Colorado State University Fort Collins, Colorado 80521 Attention: Prof. W. R. Mickelsen	1
30.	Rocketdyne 6633 Canoga Avenue Canoga Park, California 91304 Attention: J. F. Hon	1
31.	United States Air Force Office of Scientific Research Washington, D. C. 20025 Attention: M. Slawsky	1

	Addressee	Number of Copies
32.	Case Institute of Technology 10900 Euclid Avenue Cleveland, Ohio 44106 Attention: Professor O. K. Mawardi	1
33.	Case Institute of Technqlogy 10900 Euclid Avenue Cleveland, Ohio 44106 Attention: Dr. Eli Reshotko	1
34.	Astrosystems, Inc. 82 Naylon Avenue Livingston, New Jersey 07039 Attention: R. E. Wiech, Jr.	1
35.	Reaction Motors Division Thiokol Chemical Corporation Denville, New Jersey 07834 Attention: W. Courtney	1
36.	Gruman Aircraft Engineering Corporation Bethpage, Long Island, New York 11101 Attention: P. Grinoch	1
37.	The Martin Company P.O. Box 5837 Orlando, Florida 32801 Attention: Engineering Library MP30	1
38.	University of Illinois Department of Electrical Engineering Urbana, Illinois 61801 Attention: L. Goldstein	1
39.	Rocket Power Inc. 3016 East Foothill Boulevard Pasadena, California 91107 Attention: Dr. S. Singer	1
41.	Astronautical Systems Division Wright-Patterson Air Force Base, Ohio 45433 Attention: ASRMPE/R. Rivir	1
42.	Astronautical Systems Division Wright-Patterson Air Force Base, Ohio 45433 Attention: Capt. P. E. Peko (AFAPL)(APIE)	1